Supporting Information

Five-dimensional unclonable anticounterfeiting orthogonal Raman labels

Jin Li[#], Chang He[#], Haijun Qu[#], Feng Shen* and Jian Ye*

School of Biomedical Engineering, Shanghai Jiao Tong University, Shanghai, 200030, China

[#]J. Li, C. He and H. Qu contributed equally to this work.
*Corresponding authors. E-mail: feng.shen@sjtu.edu.cn (F. Shen); yejian78@sjtu.edu.cn (J. Ye)

Table of Contents

S1. Supplementary experimental procedures

S1. Supplementary experimental procedures

Materials and instrumentation. The three alkyne reporters are synthesized in our lab according to our previous work[1]. All chemicals were obtained commercially and used without further purification unless otherwise noted. Cetyltrimethylammonium chloride (CTAC, > 98.0%), acetone, ethanol and L-ascorbic acid (AA, >99.9%) were purchased from Sigma-Aldrich. Hydrogen tetrachloroaurate trihydrate (HAuCl$_4$·3H$_2$O) was purchased from Sinopharm Chemical Reagent Co. Ltd. (Shanghai, China). Ammonium fluoride, perchloric acid, sulfuric acid, and hydrogen peroxide were bought from SinoPharm Chemical Reagent Co., Ltd (Beijing, China). Hydrofluoric acid, dichlorodimethylsilane and tetradecane were bought from Innochem Technology Co., Ltd (Beijing, China). Ammonium ceric nitrate was purchased from Macklin Biochemical Co., Ltd (Shanghai, China). Soda-lime glass plates coated with chromium and photoresist, and photomasks were obtained from MicroCAD Photo-Mask LTD (Shenzhen, China). Transparent photosensitive resin (product number 4200) was purchased from Nova Robotics, Inc. (Shenzhen, China). Distilled water (18.0 MΩ cm) obtained from a Milli-Q Integral 5 system was used in all experiments. Transmission electron microscope (TEM) images were recorded on the instruments of JEM-2100F (JEOL, Japan) with an accelerating voltage of 200 kV. The surface structure of resin embedded OGERTs coated on a silicon wafer was studied by a scanning electron microscope (SEM, FEI-QUANTA 200, Holland). Extinction spectra were measured with a UV1900 UV-Vis spectrophotometer (Aucybest, Shanghai, China). Raman mapping measurements were performed on a LabRAM XploRAINV system (Horiba, China). Normal Raman and SERS spectra were acquired with a confocal Raman microscope (785 nm, 10× objective, 21 mW, and 2 s of integration time). Photocuring experiment were performed on IntelliRay UV flood curing system (Uvitron International Inc., West Springfield, MI). Bright-field images of micropatterns were acquired with a Nikon 1270 stereomicroscope (Nikon, Japan).

Synthesis of OGERTs. The preparation of OGERTs involves two main steps as follows: (1) attaching to a monolayer of orthogonal reporters onto Au cores; (2) growth of Au shell with desired thickness onto the core-reporter conjugates by adding gold salt (HAuCl$_4$) and a mild reducing agent of AA. For the synthesis of OGERTs embedded with SEE, STE and SPE (SEE OGERTs, STE OGERTs and SPE OGERTs), Au NP cores (4.7 × 10^{-10} M, 20 nm in diameter) pre-prepared according to our previous work, were first washed by centrifugation to reduce the concentration of CTAC in solution from 0.1 to 0.02 M to encourage adsorption of reporters. Then 100 μL DMF solution of reporters (4 × 10^{-3} M) was added dropwise to Au cores (2 mL) under ultra-sonication. After a period of slight stirring (8 h for each Raman reporters), the obtained solution was centrifuged and washed three times and redispersed in 1 mL CTAC solution. Finally, 480 μL ascorbic acid (4 × 10^4 M) and 800 μL reporter-modified Au cores (1.88 × 10^{-9} M) were in turn added to a mixture of 16 mL CTAC (5 × 10^4 M) and 800 μL HAuCl$_4$ (4.86 mM) rapidly under vigorous sonication to afford OGERTs in about 10 min.

Raman measurements of single OGERTs on RISE. The integrated RISE system was applied for single SPE OGERTs detection after the aqueous sample (5 × 10^{-11} M) was air-dried on a silicon wafer with some metallic marks for easier location. To avoid the damage of electron beam to NPs and Raman reporters, the monodispersed single SPE OGERTs were first identified under the bright field. Raman signals were collected from the NPs using a 785 nm laser, 100× objective lens, 2 mW laser power and 10 s acquisition time. Then, the sample was automatically transferred to the SEM chamber to confirm the distribution states of the measured NPs. The data only from single SPE OGERTs with a distance of more than 1 μm from other NPs were analyzed.

Photostability experiments. SERS photostability measurements of three OGERTs (SEE OGERTs, STE OGERTs and SPE OGERTs) were performed on solid OGERTs dropped on a silicon substrate under continuous laser (785 nm) irradiation with two different laser power densities: 2.06×10^5 and 8.24×10^5 W/cm^2 for 30 min with an integration time of 10 ms per spectrum. Brief, 10 µL samples (2×10^{-10} M) were dripped on a silicon substrate and dried before measurement. Continuous irradiation with a 785 nm laser was applied to three OGERTs. The intensity of Raman band for both types of tags was measured intermittently while exposing them to continuous laser illumination. Quantitative analysis of photostability behaviors of three OGERTs was evaluated with the integrated peak areas of Raman bands at 2104 cm^{-1} for SEE OGERTs, 2152 cm^{-1} for STE OGERTs, and 2212 cm^{-1} for SPE OGERTs. Photobleaching time constant is obtained by fitting the SERS decay curves to the equation: $I = Ae^{(-t/\tau)}$ after evaluation of three different locations on the substrate.

Fabrication and assembling of the device for SlipChip microfluidic molding. Both top and bottom plates used in SlipChip molding were fabricated from soda-lime glass plates *via* a wet etching method. The soda-lime glass plate, pre-coated with a chromium layer and a photoresist layer, was aligned with a photomask and exposed with a mask aligner system (Institute of Optics and Electronics, Chinese Academy of Sciences, Chengdu, China). After exposure, the glass plate was placed in NaOH solution (0.1 mol/L) to remove the surface of photoresist exposed to UV light. Then, the exposed chromium surface was removed by a chromium etchant solution containing 0.6 mol/L HClO$_4$ and 0.365 mol/L (NH$_4$)$_2$Ce(NO$_3$)$_6$. After thoroughly rinsing with water, the glass plate was immersed in a glass etchant solution containing HF (1 mol/L), NH$_4$F (0.5 mol/L), and HNO$_3$ (0.75 mol/L). The glass etching was performed in a shaking water bath at 40 °C to guarantee a uniform etching across the plate. When the etching process was completed, the glass plate was thoroughly rinsed with water, and then the plate was washed with EtOH to remove the remaining photoresist without exposure to UV light. The glass plate was dried and immersed back into the chromium etchant solution to remove the exposed chromium layer. After complete removal of the chromium layer, the glass plate was rinsed with water and ethanol, and then was dried. The surface of both plates was treated to be hydrophobic using the following method: the glass plate with etched pattern was oxidized in a plasma cleaner for 120 s and immediately placed in a desiccator with 25 µL of dichlorodimethylsilane. For gas-phase silanization, a vacuum was applied for 40 min. Then, the glass plate was thoroughly rinsed with chloroform, acetone, and ethanol. The top plate, with the patterned side facing down, was placed on top of the bottom plate, with the patterned side facing up. Tetradecane was placed in between two plates as a lubricant. Then the top plate and the bottom plate were aligned to have partial overlapping of the patterns on the top plate and the patterns on the bottom plate. Then, the aligned device was fixed with a clamping fixture for further label fabrication.

Manufacture of PUF labels by microfluidic SlipChip molding method. OGERTs (6×10^{-8} M) were mixed with photosensitive resins at an approximate volumetric ratio of 1:30. The mixed liquid was then introduced into the SlipChip molding device by pipetting into the inlet. After the loading was completed, the top plate was moved relative to the bottom plate to form isolated compartments. Then, the device was placed in the UV flood curing system and exposed for 5-10 s at 50 mW/cm^2, and the distance from the lamp to the device was approximately 12 cm. The clamping fixture was removed, and the top plate and the bottom plate were separated. The solidified micropatterns can be removed from the micro-cavities using tweezers, pipette tips, needles, or ultrasonic agitation.

TEM observations of NPs distribution inside resins. The sample was embedded in EPOM812 and polymerized in the oven at 60 °C for 48 h. Ultrathin sections of approximately

150 nm thick were cut at different depths of the sample using a diamond knife on a Leica UC6 ultramicrotome and transferred to the copper grid for TEM observations.

Readout of PUF labels. PUF labels with well-defined micropatterns were read *via* a confocal Raman system (LabRAM XploRA INV, Horiba) with a pinhole value of 100, 300, 500 μm under the DuoScan mode that is based on the movement of the laser spot between points. Under the DuoScan mode along with a 'SWIFT' mode, the Raman mapping speed can be significantly increased by shortening the exposure time to around 0.7 ms and only about 6 s was needed to accomplish the mapping with a resolution of 50×50 pixels. A 785 nm laser (8.24×10^5 W/cm^2, $10\times$ objective lens) was used with a 10-ms exposure time per pixel. The x-y-z SERS image was obtained by combining multiple x-y SERS images taken at various z values with predetermined intervals. To obtain x-y SERS maps at targeted z values, we first focused the laser onto the substrate base (bottom of the 3D micro-label) and define z as "0" at this position. X-y mapping at fixed z values was achieved by layer-by layer scanning with a pinhole value of 100 μm.

Digitization and authentication of PUF labels. The Raman spectrum process flow which is composed of preprocessing, classical least square (CLS) fitting and digitization was realized by MATLAB R2019a. (i) Preprocessing. A moving average method with window size of 5 and order of 3 was employed to smooth Raman spectra to suppress noises. Then the baseline correction was accomplished by the algorithm of adaptive iteratively reweighted penalized least squares (airPLS) (order = 3, lambda = 100). (ii) CLS fitting. Each Raman spectrum of the mixture is considered as a linear sum of pure component Raman spectra, including each type of OGERTs and resin. Here we used CLS algorithm to demultiplex the Raman intensity of each component in the mixture. The objective optimization function is set as:

$$min_{[W]} \frac{1}{2}\|S - R \cdot W\|^2 \tag{1}$$

where S is the measured spectrum, R is a matrix composed of n columns and each column is a spectrum of one pure component, W is a n-dimensional column vector and each element is the weight of the corresponding pure component. (iii) Digitization. After CLS fitting, the spectral data of each label was converted to a $m \times n$ matrix, m is the number of pixels and n stands for types of OGERTs. Each raw represents the intensities of OGERTs at the pixel. Since the Raman intensity will be influenced by instruments and environmental conditions, all matrices will be normalized with Z-score method by columns. Then the multi-start optimization algorithm was performed to search the common globally optimal threshold for mapping the intensity of each pixel to an element of the set {0, 1, 2, 3}. Generally, the conversion from intensity values to digital encoding can be expressed by the following formula.

$$E_{mn} = \begin{cases} 0, & I_{mn} \leq a \\ 1, & a < I_{mn} \leq b \\ 2, & b < I_{mn} \leq c \\ 3, & I_{mn} > c \end{cases} \tag{2}$$

I_{mn} and E_{mn} are the Raman intensity and digitization value of the pixel in the mth row and nth column, respectively. The a, b, and c are the three thresholds calculated by the multi-start algorithm. The aim of multi-start optimization algorithm is to find the best threshold to obtain highest reproducibility for same label and lowest reproducibility for different labels. Objective optimization function is set as:

$$\max \sum_{i=1}^{N} \sum_{j=i+1}^{N} sign(label_i, label_j) \times \frac{Match(label_i, label_j)}{M} \tag{3}$$

$$sign(label_i, label_j) = \begin{cases} -1, & if\ label_i\ and\ label_j\ are\ different\ labels \\ +1, & if\ label_i\ and\ label_j\ are\ same\ label \end{cases} \tag{4}$$

4

where N is the number of matrices, $Match(label_i, label_j)$ is the pixel number with same digitization value between $label_i$ and $label_j$ and M is the number of pixels of the matrix. Here we collected three measurements for 46 labels. The 32 of these labels were used to search the threshold for digitization by the MS algorithm and the other 14 labels were used to verify the threshold is reliable. Here, N in the (2) is $46 \times 3 = 138$. After finding the threshold, we calculated similarity index I of 138 comparisons of same label and 5283 comparisons of different labels. The similarity index I is defined as:

$$I = \frac{Match(label_i, label_j)}{M} \tag{5}$$

Calculation of 3D autocorrelation coefficient. In this work, we employed Geary's C coefficient to evaluate spatial autocorrelation of the digital bits of the PUF labels, which is defined as.

$$C = \frac{(N-1)}{2K} \cdot \frac{\sum_{i=1}^{N}\sum_{j=1}^{N} w_{ij}(z_i - z_j)^2}{\sum_{i=1}^{N}\sum_{j=1}^{N}(z_i - \bar{z})^2} \tag{6}$$

where w_{ij} can be expressed as,

$$w_{ij} = \begin{cases} 1 & if\ i\ and\ j\ are\ neighbors \\ 0 & if\ i\ and\ j\ are\ not\ neighbors \end{cases} \tag{7}$$

the K is the number of neighboring elements, which can be expressed as

$$K = \sum_{i=1}^{N}\sum_{j=1}^{N} w_{ij} \tag{8}$$

the z_i and z_j represent the values of the bits at the ith and jth location in PUF keys, $\bar{z}$ is the mean value of bits, N= 2500 is the number of bits. The analysis was performed by considering six most neighboring bits illustrated in Figure S13. The Geary's C index ranges from 0 to 2. C = 1 means no spatial correlation. The average Geary's C coefficient for ten disk-based PUF labels was determined to be 0.9448, which means nearly no correlation between neighboring bits.

Fabrication of a disk-over-rectangle label by the slip overmolding method. We fabricated a two-layer disk-over-rectangle label by the slip overmolding method. The first and second raw materials consist of resins, resins embedded with SPE OGERTs, respectively. The top and bottom plates consisted of microfluidic ducts and microcavities with different shapes, and a lubricating oil was placed between the two plates. The top and bottom plates were assembled into the first position where the bottom plate circular wells partially overlapped with the microfluidic ducts on the top plate, and the first liquid-form raw material consisted of resins was introduced into the device. Then, the top plate was manually moved up relative to the bottom plate to the second position where the first liquid-form raw material was compartmentalized into the rectangle microcavities and solidified to form the rectangle base layer. In the second position, the ring-shaped microcavities on the top plate and fluidic ducts on the bottom plate were partially overlapped, and the second liquid-form raw material consisted of resins embedded with SPE OGERTs was injected into the device. Then, the top plate was moved up relative to the bottom plate to the third position where the ring microcavities were disconnected from the ducts on the bottom plate and overlapped with the circular microcavities on the bottom plate containing the solidified first material; the second material was then allowed to solidify to form an overmolded layer. Finally, the top plate was removed, and the two-layer disk-over-rectangle label can be harvested.

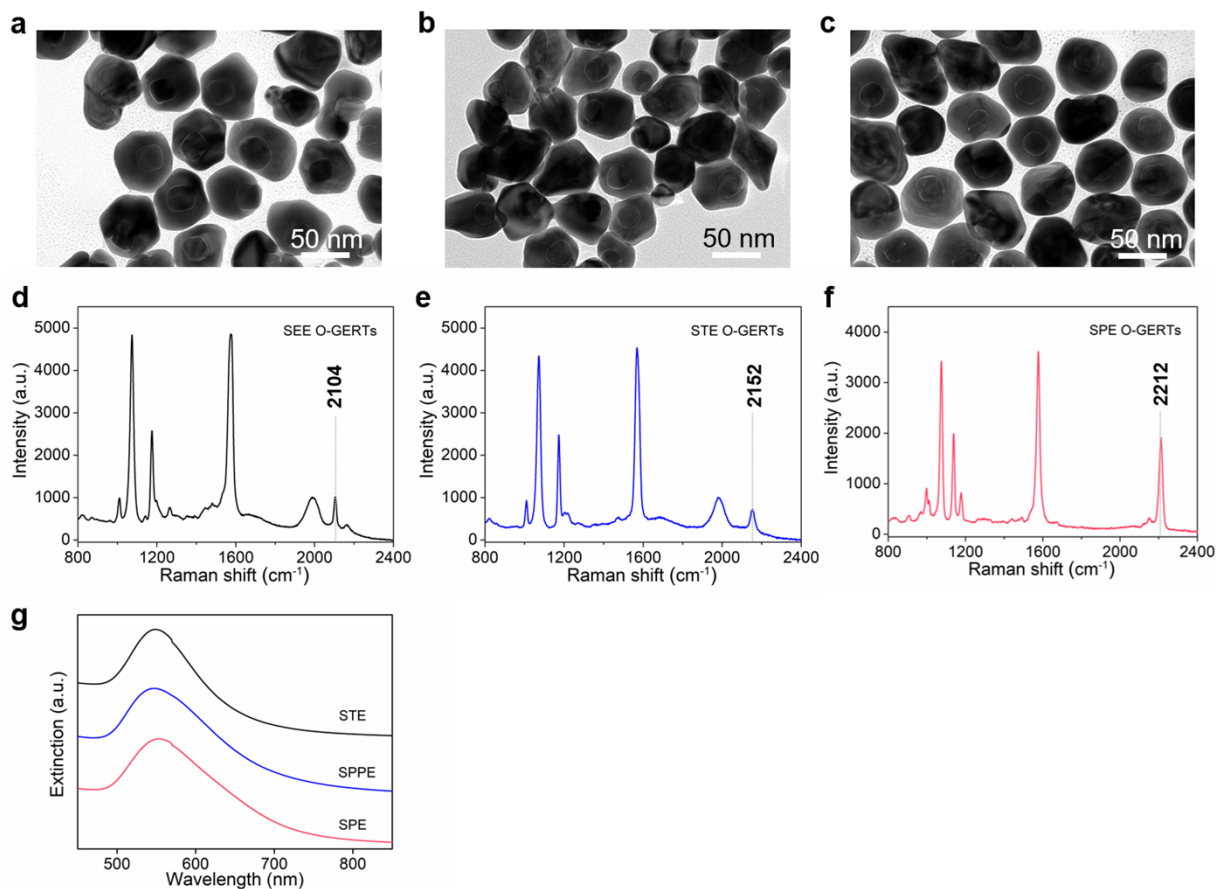**S2. Supplementary Figs. S1-S15, Table S1-S2**

Figure S1. Characterization of three types of OGERTs. (a-c)TEM images of SEE OGERTs, STE OGERTs and SPE OGERTs. (d-f) Raman spectra of SEE OGERTs, STE OGERTs and SPE OGERTs upon 785 nm NIR excitation. (g) Extinction spectra of SEE OGERTs, STE OGERTs and SPE OGERTs.
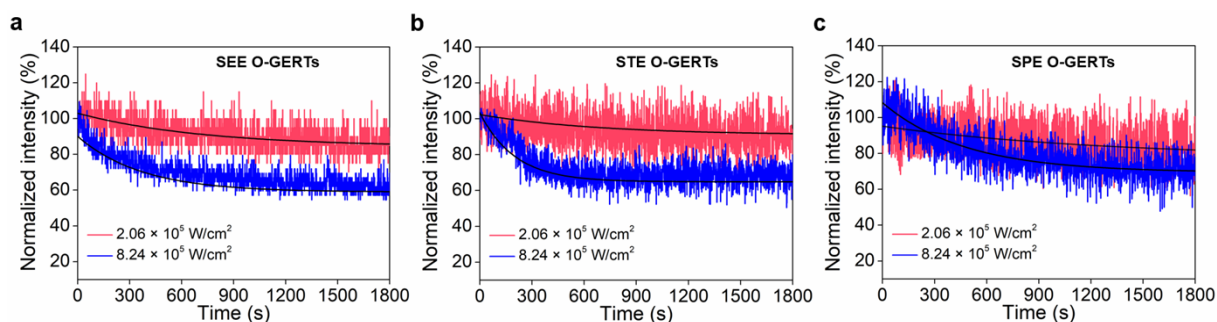
Figure S2. Photostability of SEE OGERTs (a), STE OGERTs (b) and SPE OGERTs (c) under laser power density of (red) 2.06×10^5 and (blue) 8.24×10^5 W/cm^2 with 785 nm laser. Photostability of the three OGERTs were evaluated with integrated peak areas of Raman-silent bands (2104 cm^{-1} for SEE OGERTs, 2152 cm^{-1} for STE OGERTs, 2212 cm^{-1} for SPE OGERTs) under continuous laser irradiation with different power densities for 30 min. Through quantitative analysis of photobleaching behaviors of time-resolved SERS trajectories, we found that the photobleaching time constant is 726 s for SEE OGERTs, 692 s for STE OGERTs, and 1291 s for SPE OGERTs under 2.06×10^5 W/cm^2, while the value is 369 s, 202 s and 473 s under 8.24×10^5 W/cm^2, respectively. The ultrahigh photostability of OGERTs is mainly due to the reasons including: 1) the solid metallic shell well protects the built-in alkyne reporters to avoid possible desorption and minimizes photoinduced chemical reactions by isolation from the environment (oxygen, moisture, etc.); 2) the use of off-resonance laser excitation in the NIR region (e.g., 785 nm) circumvents the plasmon resonance of OGERTs in the visible region (e.g., 540 nm in Figure S1g), which dramatically reduces the photoheating effects from the laser.
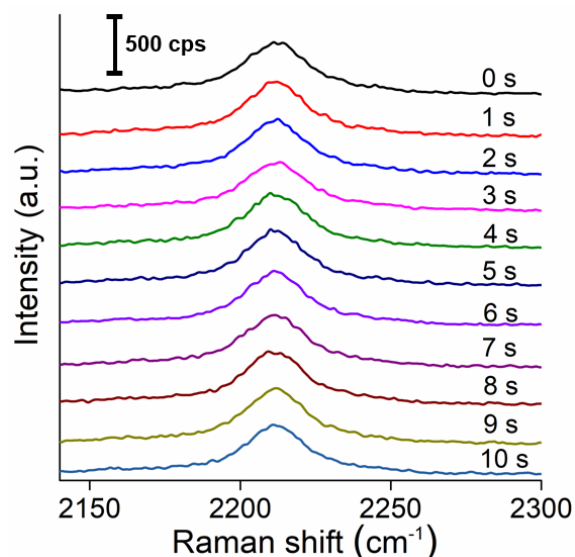
Figure S3. Time-course Raman spectra of SPE OGERTs in ten seconds when irradiating the solid OGERTs sample with 785 nm laser under laser power density of 8.24×10^5 W/cm^2. If the label goes through 1000 repeated authentications, the total time of laser irradiation on one pixel is only 10 s. We therefore extracted the time-course Raman spectra in ten seconds, during which the intensity loss of the OGERTs can be ignored.
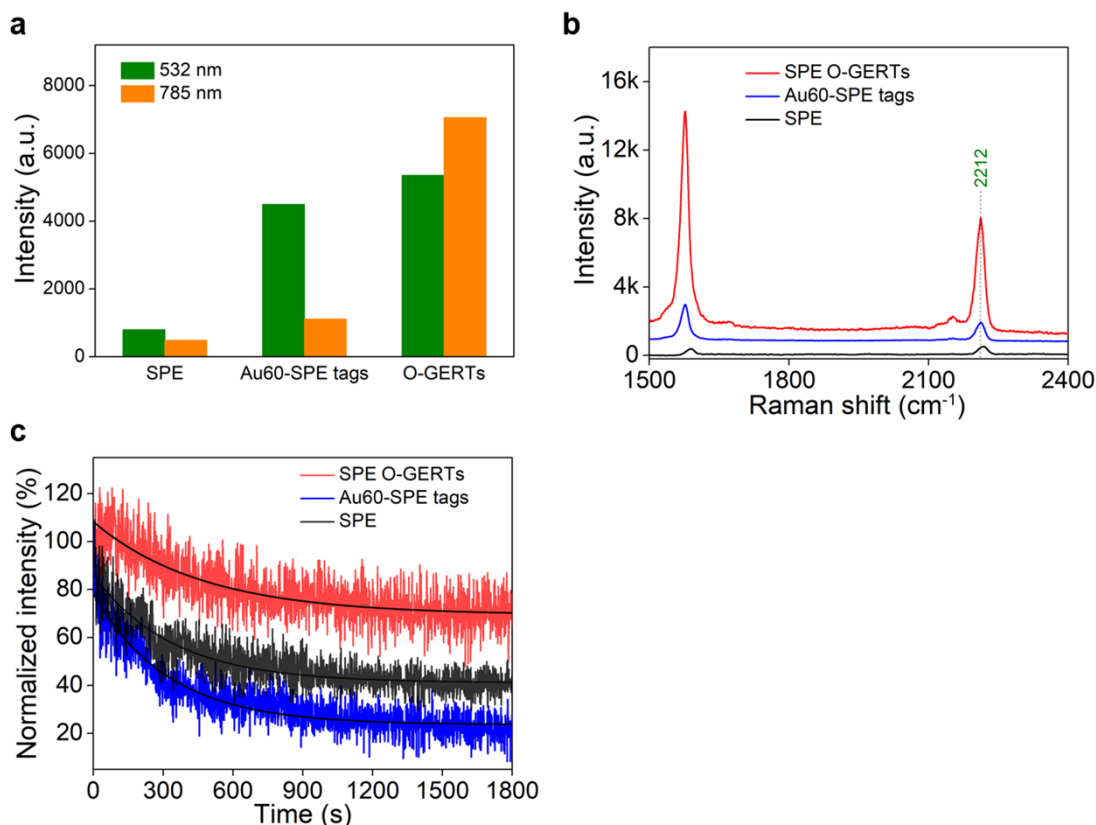
Figure S4. Comparison of intensity and photostability for three types of Raman tags. (a) Signal intensity (2212 cm^{-1}) comparision of SPE molecules, conventional (Au60-SPE) SERS tags and SPE OGERTs excited by 532 nm and 785 nm laser. Gold nanoparticles (60 nm in diameter) with SPE molecules in the surface, termed as Au60-SPE tags, were chosen as conventional SERS tags. The concentration of SPE molecules, Au60-SPE tags and SPE OGERTs is 10 mM, 0.3 nM and 0.3 nM, respectively. Unlinke Au60-SPE tags, these OGERTs exhibit stronger signals upon NIR excitation than those with visible light excitation at 532 nm, due to a combination of electromagnetic field enhancement and electron transport effect across molecular layer in the nanogaps.[2] (b) Raman spectra of SPE molecules, Au60-SPE tags and SPE OGERTs excited by 785 nm laser. Raman measurements were performed using a 785 nm laser, 20 mW power, 2 s acquisition time, and 10× objective lens. (c) Photostability of SPE molecules, Au60-SPE tags and SPE OGERTs under the laser power density of 8.24×10^5 W/cm^2. Photostability of three types of were evaluated with integrated peak areas of Raman band at 2212 cm^{-1} for both tags under continuous laser irradiation with different power densities for 30 min.
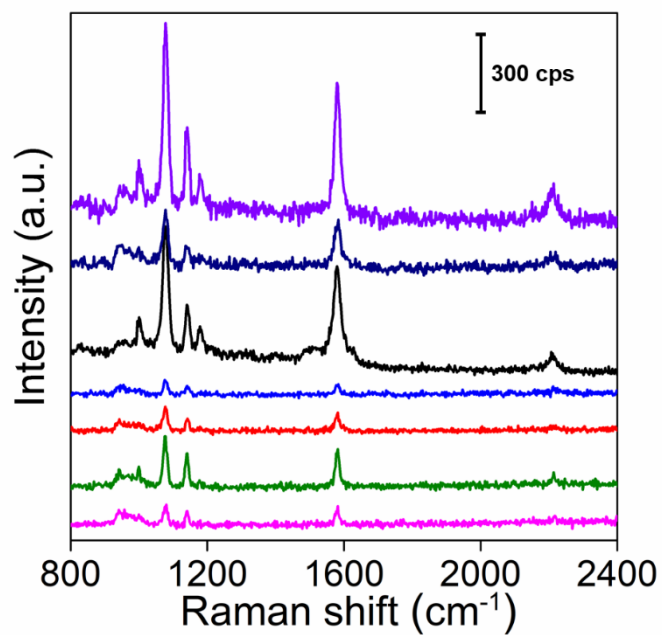
Figure S5. SERS spectra of the other seven single SPE OGERTs measured using the RISE system.

Table S1. Summary of intensity and photostability for three types of Raman tags upon 785 nm excitation

Tags	Intensity in the silent regime	Photobleaching time constant
SPE molecules	481	340 s
Au60-SPE tags	1110	320 s
SPE OGERTs	7052	473 s
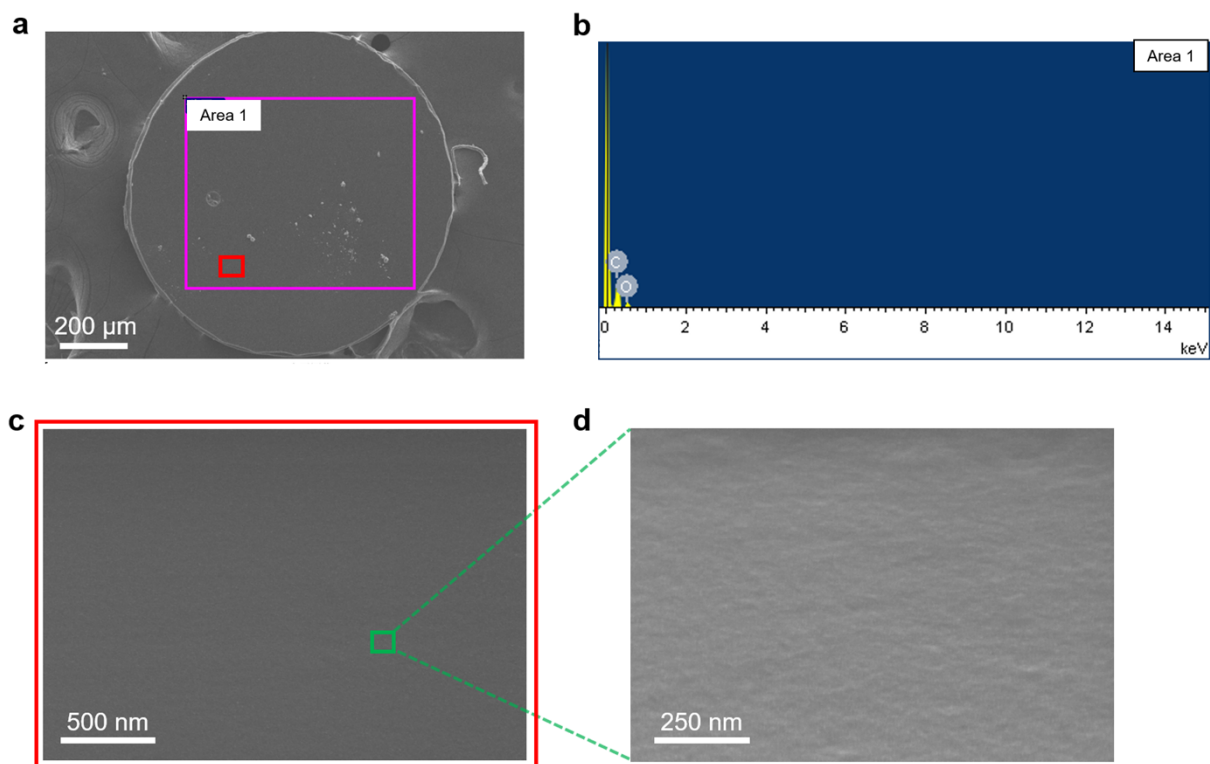
Figure S6. SEM and EDS characterization of a disk-based PUF label. (a) SEM images of the PUF label. (b) EDS spectra of area 1 labelled in the panel A. (c) SEM images of the label marked in the panel A. (d) Zoom-in SEM images of the label marked in the panel c.
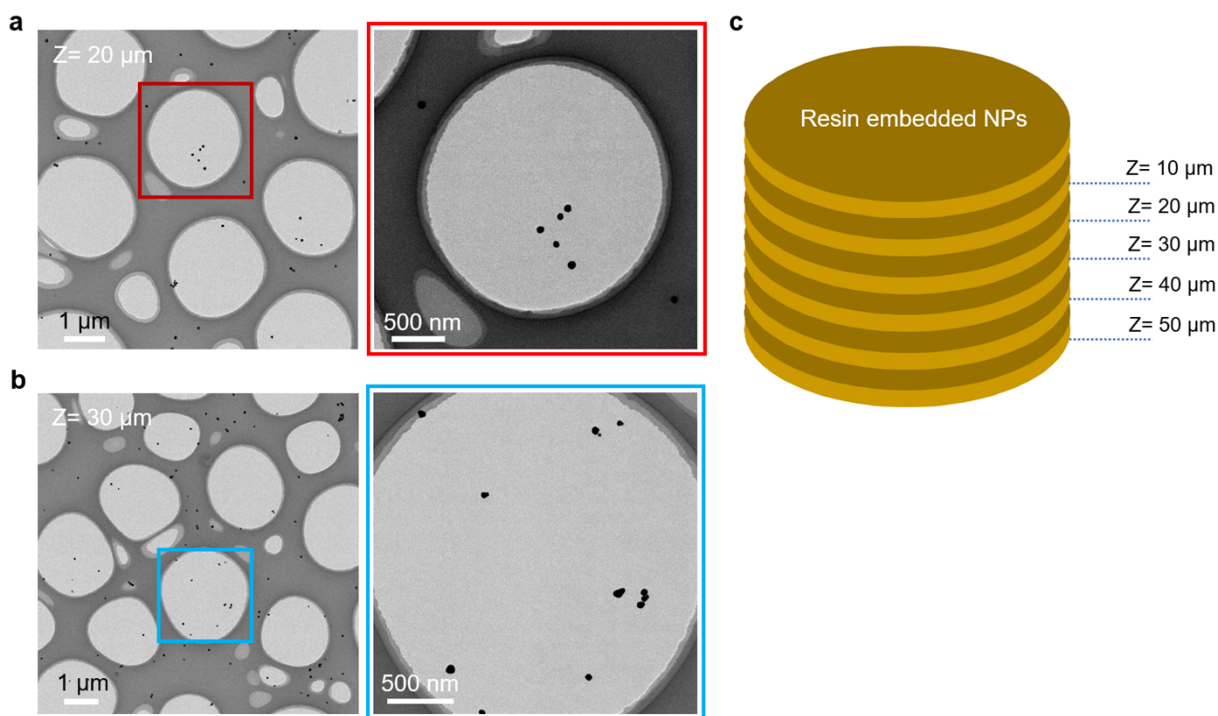
Figure S7. TEM images from ultrathin sections of the disk-based PUF label. (a-b) Representative TEM images from ultrathin sections of the PUF label at the depth of (a) 20 μm and (b) 30 μm. (c) Schematic representation of the PUF label with a thickness of 50 μm for ultra-thin section sample preparation. The sample is first placed in a pyramid-shaped container filled with EPOM812 for polymerization. After complete polymerization, the sample is encapsulated in a pyramid-shaped polymer mold. Then, the mold is fixed on a Leica UC6 ultramicrotome for guiding the sample direction for cutting. Thus, we can obtain slices of different depths of the sample with a diamond knife.
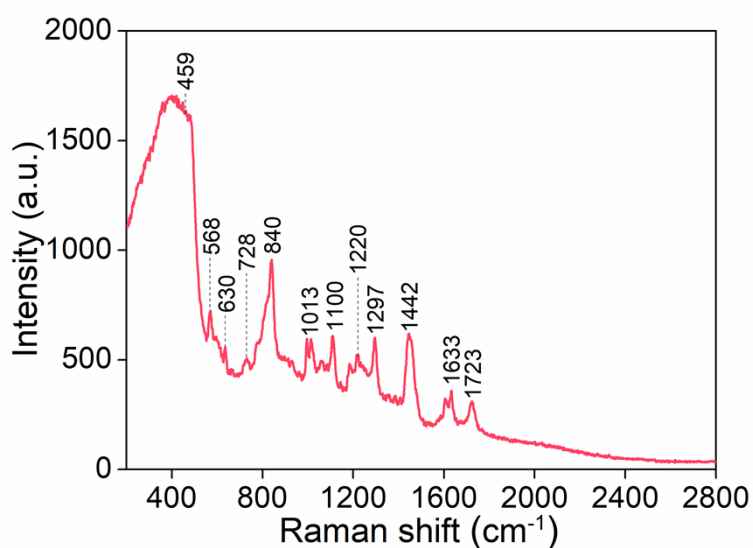
Figure S8. Raman spectrum of the photo-crosslinked resin excited by 785 nm laser.

Table S2. Assignment of typical Raman bands of the resin [3-5].

Raman bands (cm^{-1})	Assignments
459	γ(C-C-C)
568	γ(C−C−H) ring bend
630	γ(C-C-C)
728	γ(C-H)
842	-CH$_3$ groups (several vibrational modes)
1013	Benzene ring breathing
1100	ν(C-C), backbone stretches
1220	ν(C-O-C)
1297	ν (C-S)
1442	δ(CH$_2$), CH$_2$ scissors bending
1633	ν(C=C), cis stretch
1723	ν(C=O), C=O esters
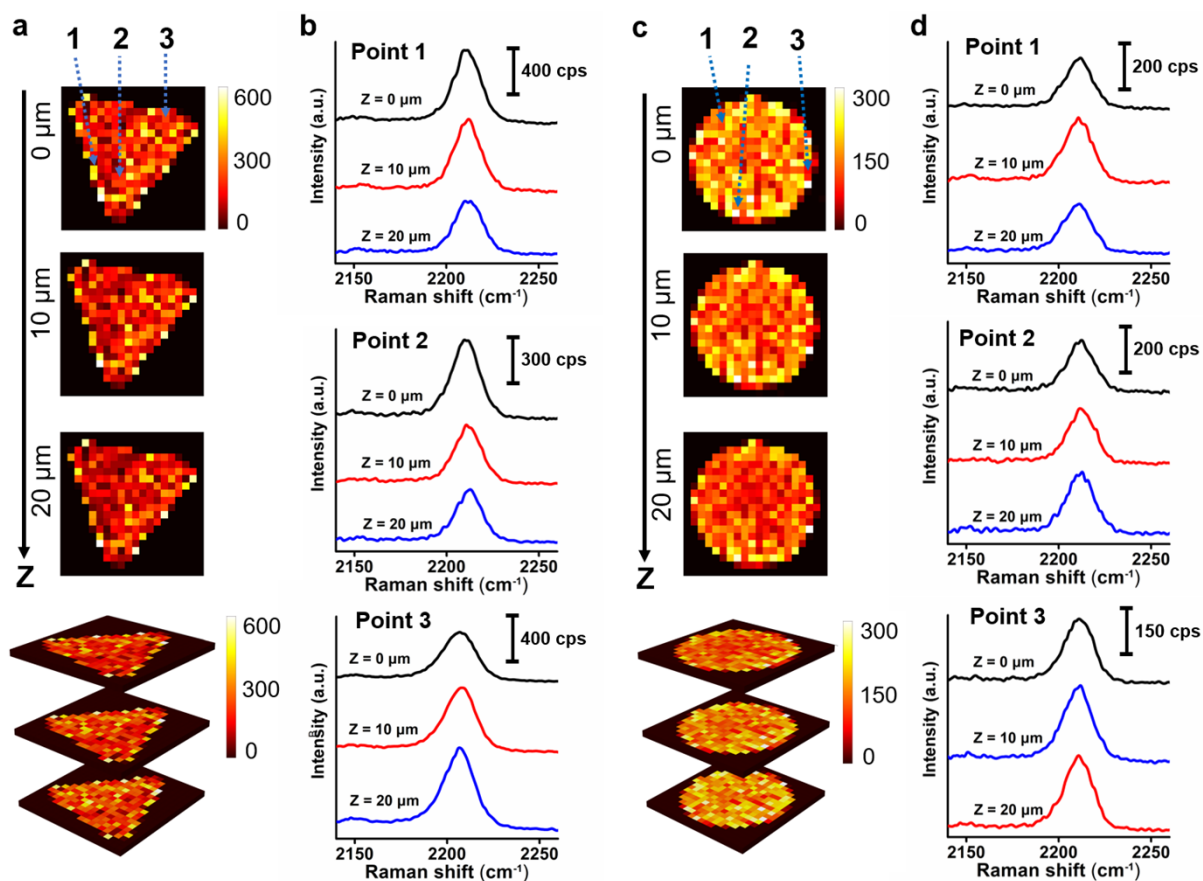
Figure S9. Raman mapping of the triangle- and disk-based PUF labels. (a) (top) 2D Raman images at various *z* positions from 0 to 20 μm of a triangle-based label and (bottom) the corresponding 3D plotting. (b) Raman spectra of thr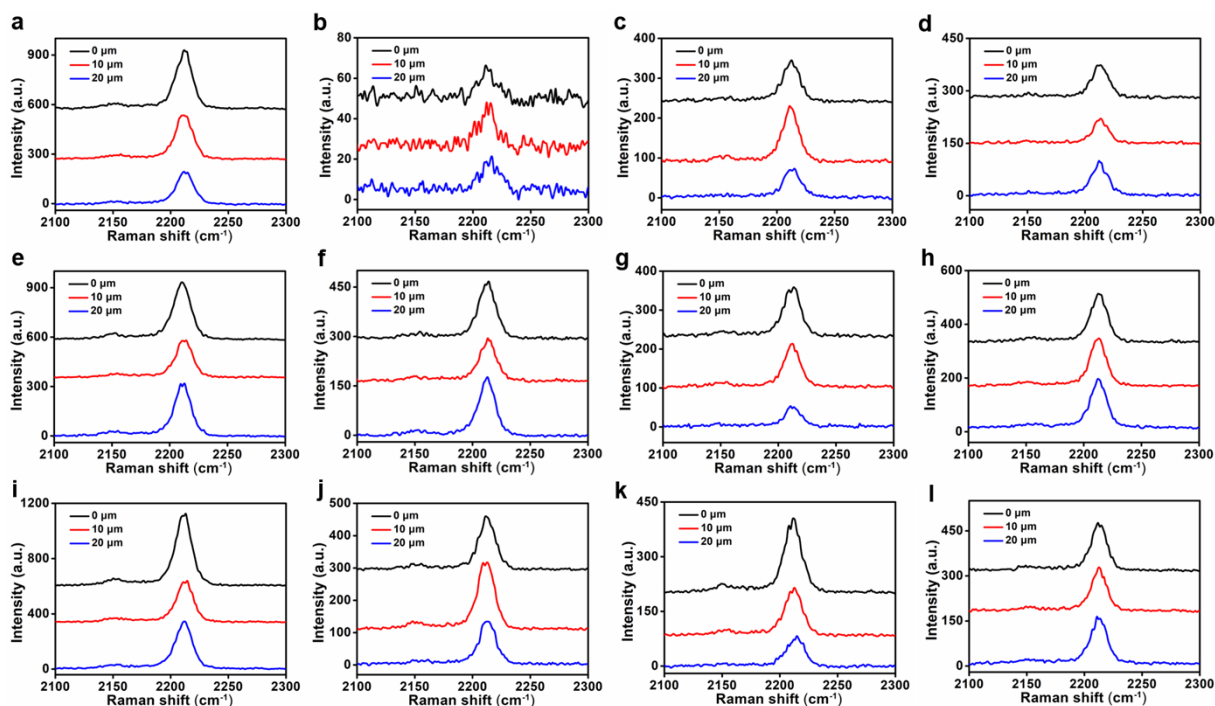ee points extracted from the triangle-based PUF label. (c) (top) 2D Raman images at various *z* positions from 0 to 20 μm of a disk-based label and (bottom) the corresponding 3D plotting. (d) Raman spectra of three points extracted from the disk-based PUF label.

Figure S10. Raman spectra of 12 points extracted from the square-based PUF label. (a-l) Raman spectra of the square micropattern-based PUF labels embedded SPE-OGERTs showing that the SERS intensities of the 2212 cm^{-1} band on the micropatterns are stochastic between different points at the same layer and different layers at the same points.
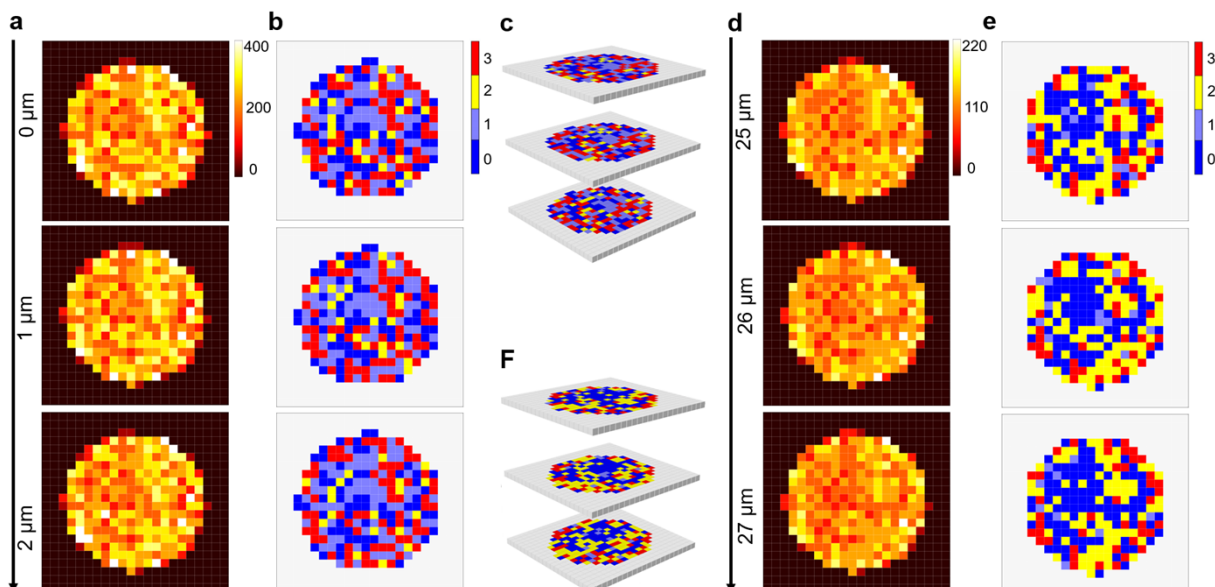

Figure S11. Quaternary encoding of a disk-based PUF labels with an interval of 1 μm along z axis. (a-c) Raman mapping and digitization of the labels with the z-position from 0 to 2 μm and the corresponding 3D digital plotting. (d-f) Raman mapping and digitization of the labels with z-position from 25 to 27 μm and the corresponding 3D digital plotting.
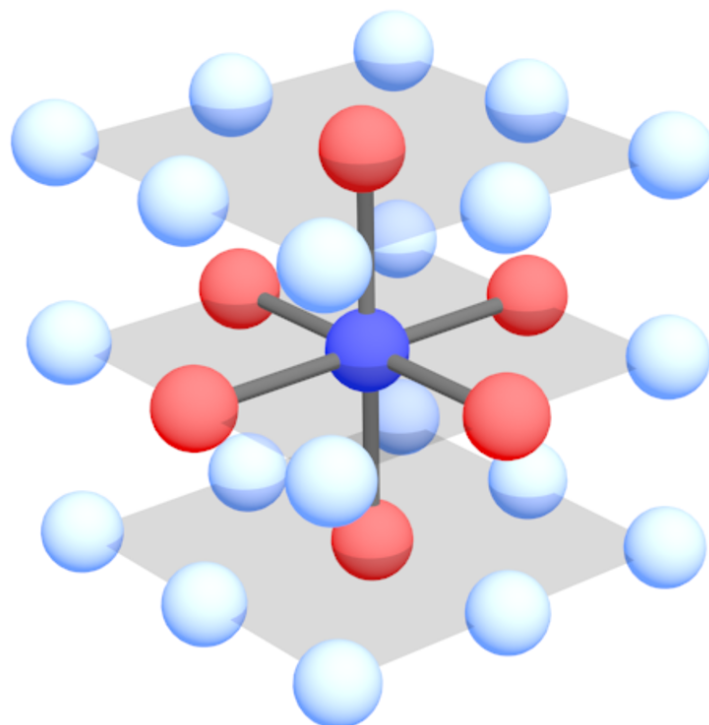
14

Figure S12. Schematic representation of spatial distribution of bits in three-layer digital codes of the PUF labels for 3D autocorrelation coefficient analysis. Balls represent bites. The six red balls represent six most neighboring bits around to the blue one.

Table S3. Comparison of Raman anticounterfeiting labels encoded with three and five dimensions

Properties	Three dimensional labels	Five dimensional labels
Randomness (Geary's C coefficient)	1.3358	0.9528
Encoding capacity	1.4×10^{360}	1.1×10^{5852}
Information density (Tbit/cm³)	5.2×10^{382}	4.0×10^{5844}
Key size (bit)	1296	19440

The comparison was performed on the "key" micropattern security labels with three dimensions (2D spaces, intensity, one color) and five dimensions (3D spaces, intensity, three color). The Randomness was performed through spatial autocorrelation analysis by calculating Geary's C coefficient. The Geary's C index ranges from 0 to 2. C = 1 means no spatial correlation. The Geary's C index is far away from 1, indicating the decrease of randomness.
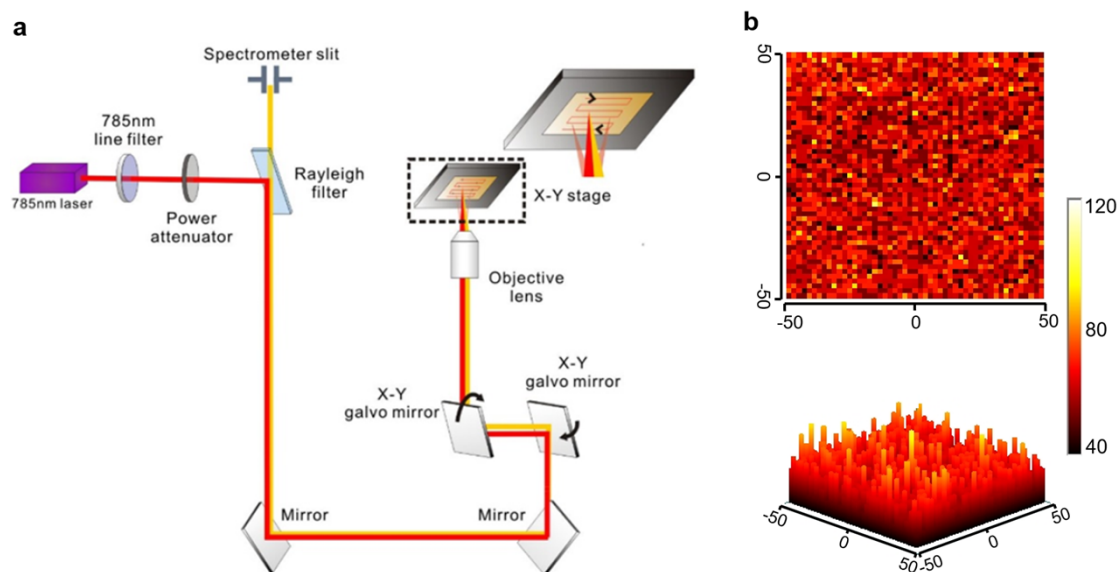
Figure S13. High-speed readout of PUF labels fabricated using SPE OGERTs embedded inside resins. (a) Schematic of configurations of Raman system used for high-speed scanning. Under the DuoScan mode, two galvo mirrors rotate along two orthogonal axes in the mirror plane, controlling movements of the laser spot along the X and the Y axis, respectively. (b) 2D (top) and 3D (bottom) plot for a PUF label (100×100 μm^2) read in DuoScan mode in 6 s with a resolution of 50×50 pixels. The Raman image is plotted using the Raman band (2212 cm^{-1}) of SPE OGERTs.
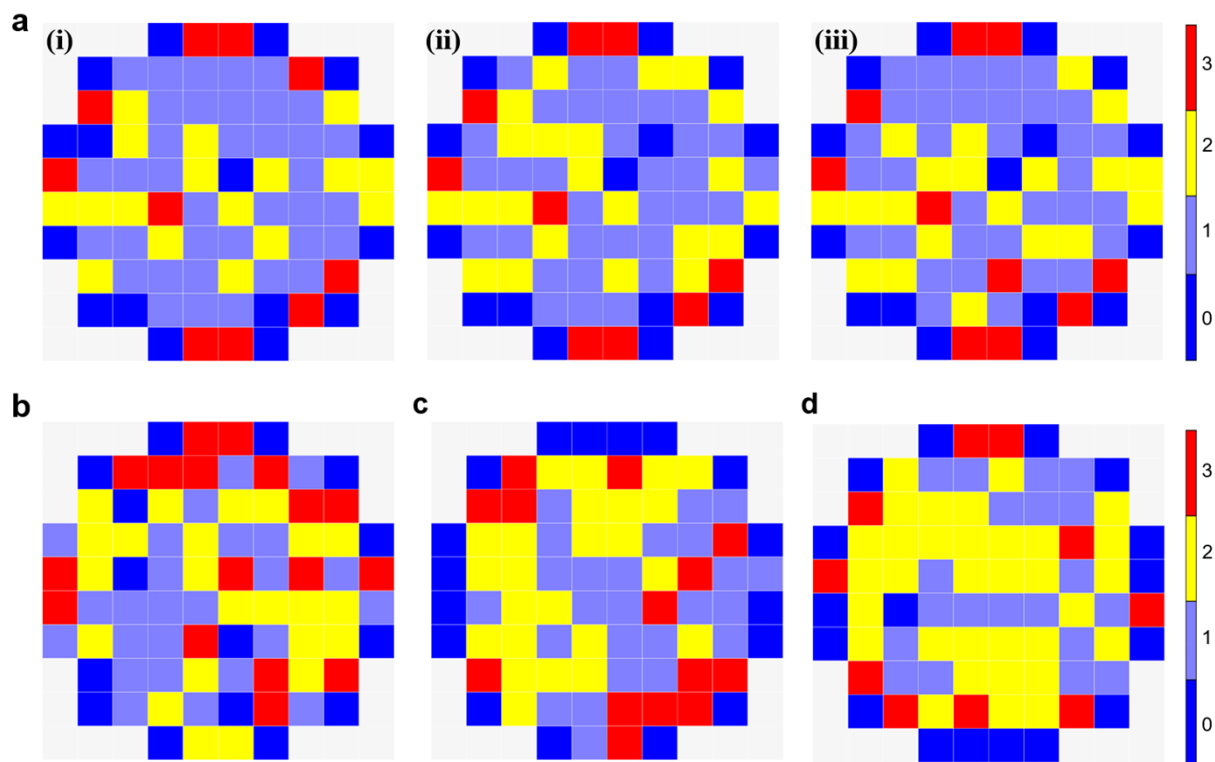
Figure S14. Reproducibility evaluation of four disk-based PUF labels. (a) A disk-based PUF label embedded SPE OGERTs is read with a resolution of 10 × 10 pixels and digitized with quaternary encoding of Raman intensity levels (2212 cm^{-1}) at each pixel for the first (left), second (middle), and third (right) measurements. Digitization of additional three different labels numbered 2 (b), 3 (c) and 4 (d) for d quaternary encoding of Raman intensity levels at each pixel with a resolution of 10 × 10 pixels.
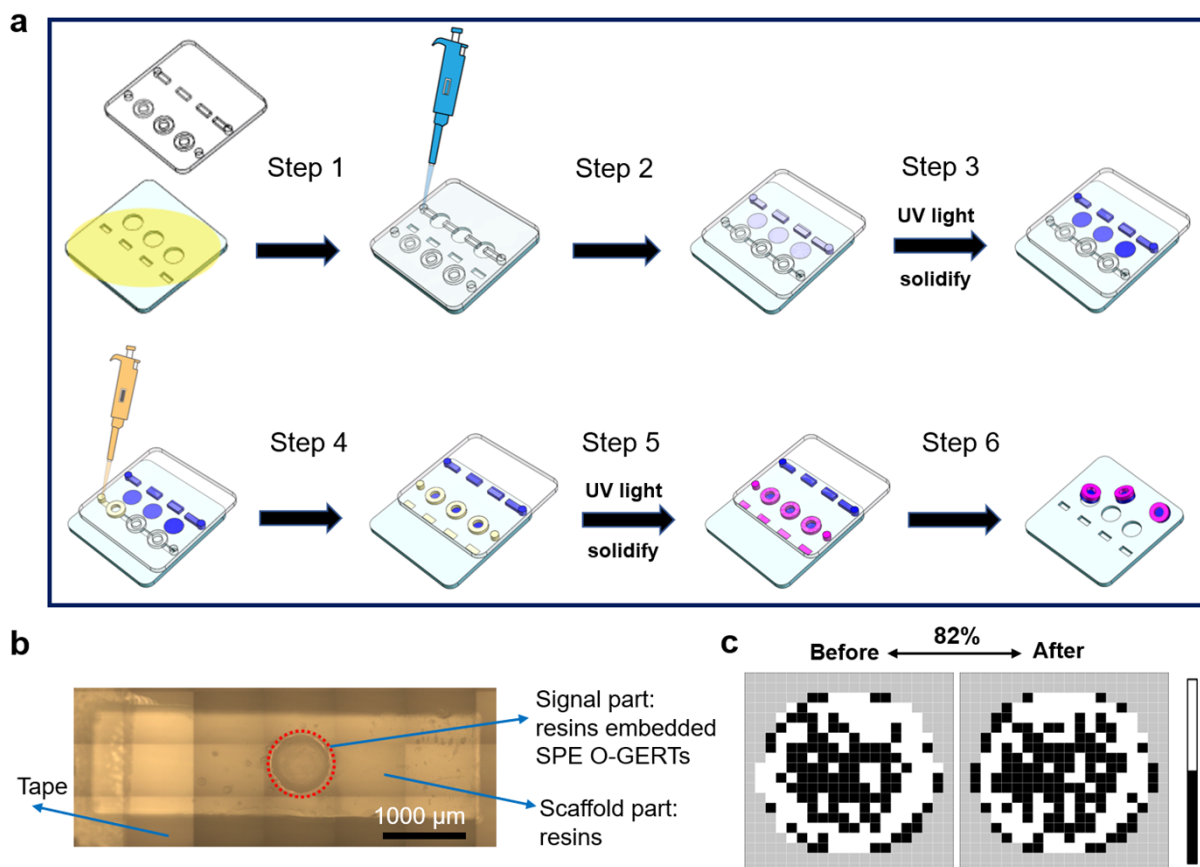
17

Figure S15. (a) Schematic representation of the fabrication procedure of two-layer PUF labels by the slip overmolding method: (step 1) introduction of the assembled slip overmolding device and the first liquid-form material (baby blue) into the device; (step 2) moving up of the top plate relative to the bottom plate; (step 3) solidification of the first material (blue); (step 4) introduction of the second liquid-form material (light orange) into the device, and moving up of the top plate relative to the bottom plate; (step 5) solidification of the second material as the second layer of mPods (pink); (step 6) removal of the top plate and harvesting of the two-layer PUF labels. (b) Photograph of the two-layer label with a disk-over-rectangle shape. The tape labelled in panel B is used to fix the label and facilitate bending experiments. (**c**) The digitized binary codes from the labels before and after 20 mechanical stress cycles. Digitized codes are derived using the 2212 cm^{-1} vibrational band of SPE OGERTs.

Supplemental references

1   J. Li, H. Liu, P. Rong, W. Zhou, X. Gao and D. Liu, *Nanoscale*, 2018, **10**, 8292-8297.
2   L. Lin, Q. Zhang, X. Li, M. Qiu, X. Jiang, W. Jin, H. Gu, D. Y. Lei and J. Ye, *ACS Nano*, 2018, **12**, 6492-6503.
3   R. A. Alvarez-Puebla, D. S. Dos Santos Junior and R. F. Aroca, *Analyst*, 2004, **129**, 1251-1256.
4   F. Madzharova, Z. Heiner and J. Kneipp, *J. Phys. Chem. C*, 2020, **124**, 6233-6241.
5   S. R. Smith and J. Lipkowski, *J. Phys. Chem. C*, 2018, **122**, 7303-7311.